

Quantum chaos induced by scaled disorder

J. A. Vergés

Instituto de Ciencia de Materiales de Madrid, Consejo Superior de Investigaciones Científicas, Cantoblanco, E-28049 Madrid, Spain

E. Louis

Departamento de Física Aplicada, Universidad de Alicante, Apartado 99, E-03080 Alicante, Spain

(Received 23 November 1998)

Quantum chaos is obtained for a two-dimensional square lattice with a number of vacancies that scales with the linear size of the cluster L . The appearance of quantum chaos is signaled by both level and wave function statistics. Since states are extended, ballistic transport behavior is expected. In particular, we show that the static conductance increases linearly with L . [S1063-651X(99)51104-5]

PACS number(s): 05.45.Mt, 73.20.Dx, 03.65.Sq

The statistical properties of measurable magnitudes of mesoscopic systems play an important role in the physics of mesoscopic phenomena [1,2]. Random matrix theory (RMT) [3] has been successfully used to explain most of the experimentally known statistical results. The nonlinear supersymmetric σ -model demonstrates the relevance of RMT in slightly disordered systems [4] and makes detailed predictions for some deviations [5]. However, generalization of these results to chaotic *ballistic* systems brings technical complications, since average over disorder should be substituted by energy averaging of an action in which the Liouville operator replaces the diffusion operator. Alternatively, one can study disordered systems that are nevertheless ballistic from the point of view of their transport properties. A billiard having a rough surface is the model of choice [6,7]. Other possible models are distorted integrable billiards [8]. Following this idea, Blanter, Mirlin, and Muzykantskii have presented a detailed supersymmetric study of the statistical properties of rough circular billiards [9]. The level statistics for the same problem was studied by Tripathi and Khmelnitskii [10]. Motivated by the important differences between systems having surface or bulk disorder, we have further analyzed our original model [7] in order to unravel the relevant parameters. It happens that the crucial characteristic is not the physical placement of defects but their number, or more precisely, the scaling of the number of defects as the size of the system grows. If the ratio between the number of defects and the billiard area, i.e., the defect density, is constant, transport properties of the system scale from the diffusive regime towards localization at large enough size scales. At the same time, statistical properties scale from Wigner-Dyson behavior to Poisson statistics. On the other hand, if the number of defects is proportional to the number of surface sites, i.e., defect density is inversely proportional to linear size, transport properties are ballistic *at all size scales* (see below). Diffusive or localized transport behavior is never reached. Statistical properties are well described by RMT at any system size. Moreover, the detailed distribution of defects over the billiard does not matter. In this way, we arrive at the simplest model showing chaotic statistics and ballistic transport properties: a square cluster of side L with a number of vacancies of order L placed at random positions.

The model of a quantum chaotic billiard presented in this Rapid Communication is not only the more general one possible but also simpler than the original one because the substitution of defects by vacancies eliminates one unnecessary technical complication. Nondiagonal or topological disorder occupies the place of diagonal disorder, eliminating one irrelevant parameter from our model, the width of the distribution of diagonal energies. Only one energy scale remains, the one defined by the hopping integral. The other superfluous characteristic of our former billiard model was the placement of all the defects on the surface of the system. We were modeling roughness in a practical implementation but here we show that bulk roughness in the form of forbidden places is also valid. In other words, what matters is just the relationship between forbidden and allowed sites but not their relative spatial distribution.

Our model of a quantum billiard is described by means of a tight-binding Hamiltonian with a single atomic level per lattice site,

$$\hat{H} = - \sum_{i,j_i} \hat{c}_i^\dagger \hat{c}_{j_i}, \quad (1)$$

where the operator \hat{c}_i destroys an electron on site i , all the hopping integrals are taken equal to -1 and restricted to nearest neighboring sites. j_i gives just the labels of the existing nearest neighbors of site i . Periodic boundary conditions are used for the study of spectral properties in order to minimize finite size effects. Therefore, the difference between our Hamiltonian \hat{H} and the one corresponding to an ideal $L \times L$ cluster of the square lattice is the absence of hopping to and from L sites chosen at random among the L^2 sites defining the lattice. Spectral calculations have been carried out on clusters of linear sizes up to $L = 100$, whereas conductance has been measured up to $L = 500$.

The classical analog of our model shares some features with the pinball game. Certainly, a classical $L \times L$ table including about L/a circular scatterers of linear size a centered at random positions shows classical hard chaos. Notice that our model is characterized by two length scales: a microscopic one equal to a and a mesoscopic one given by L . Scaling towards chaos requires a number of defects (scatter-

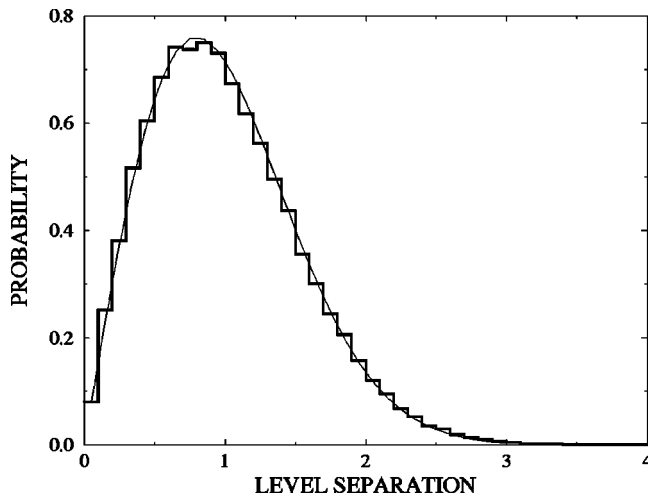


FIG. 1. Nearest-neighbor statistics obtained for 25 samples of 100×100 billiards compared to the Wigner-Dyson distribution. Level separation is given in units of the mean level separation.

ers) of order L/a , i.e., just the ratio between length scales. This is a basic characteristic discussed in our previous model on a general quantum-mechanical billiard [7]. Alternatively, our model can be described as a billiard having internal surfaces limiting forbidden areas instead of just one surface bounding the overall particle movement. Therefore, our quantum model is not very far from standard classical billiards, such as Bunimovich stadium or Sinai once a superficial first sight is substituted by a somewhat closer analysis. Random placement of vacancies is equivalent to a random shape of the internal surface, and this is the stronger justification of calling our model the more general quantum billiard model.

We follow standard quantum mechanical analysis of our model in order to show the existence of chaos [11]. We obtain spectral and wave function statistics and show good agreement with random matrix theory (RMT). Eigenvalues of one hundred samples of 50×50 clusters and 25 samples of 100×100 systems (250 000 levels) have been collected. Nearest-neighbor statistics has been computed for the states between energies -2.2 and -0.5 for both sets of eigenvalues. Remember that the spectrum lies between -4 and 4 for our model and is symmetric about 0 since the lattice is bipartite. Results are shown in Fig. 1. Accordance with the Wigner-Dyson distribution corresponding to the Gaussian orthogonal ensemble (GOE) is excellent and independent on the system size. Level repulsion, spectrum rigidity, etc. are implied by this result, which is the standard hallmark of quantum chaos. Nevertheless, other statistics, such as the variance of the number of states in an energy window of variable width is a deeper measure of the spectral properties. Figure 2 shows our results for the two sets of data together with GOE prediction. The energy range covered is exactly the same as previously, i.e., a major part of the whole spectrum. We see that results are now slightly size dependent and differ qualitatively from RMT prediction.

Certainly, GOE statistics is followed for energy windows extending over a small number of eigenvalues, whereas calculated fluctuations are sensibly smaller and almost equal to 1 for larger energy windows. This result was previously found for our rough billiard model and theoretically ex-

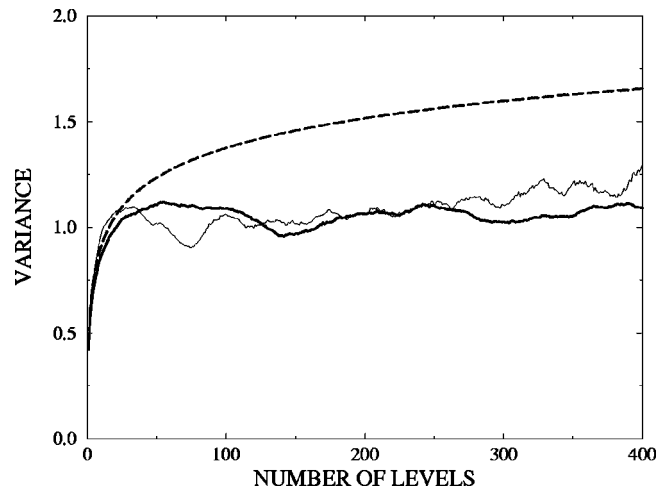


FIG. 2. Number variance obtained for 100 samples of 50×50 systems (thin line) and 25 samples of 100×100 billiards (thick line) compared to the standard GOE result (broken line).

plained by Blanter, Mirlin, and Muzykantskii [9]. Both the saturation value and the small oscillations about that value allow a closer comparison with the ballistic σ -model predictions. The period of the oscillations increases with $L = \sqrt{N}$, N being the number of sites (i.e., proportional to the number of levels up to the Fermi energy) as predicted by Blanter, Mirlin, and Muzykantskii and expected for a generic chaotic billiard [12]. Nevertheless, the saturation value does not seem to depend on N as predicted by Eq. (15) of Ref. [9].

Let us now turn to the statistical properties of wave functions. Owing to the use of periodic boundary conditions, finite size effects are minimized and both participation ratio and its fluctuation closely follow RMT predictions for matrices of comparable sizes. Squared wave function amplitude statistical distribution should follow the corresponding Porter-Thomas law according to 0D supersymmetric nonlinear σ model results [4]. Figure 3 shows the wave function probability results obtained for all eigenstates between the one being number 6923 and the one being number 7692 in a 100×100 billiard with a variable number of vacancies. These numbers do not have any physical meaning; it is just a nonbiased form of selecting a relevant part of the whole set of eigenstates. We see that GOE prediction is closely followed over more than five decades when the number of vacancies is of order 100 (the linear size of the system) but clearly differs from it both for smaller and larger number of defects. Actually, the distribution is narrower for a smaller concentration of vacancies, whereas it shows a significantly enhanced tail when the number of defects is proportional to the cluster area. These results have a straightforward explanation. Almost ordered systems are characterized by Bloch wave functions having spatial uniform probability. This would imply a δ -like distribution. Nevertheless, many states are degenerate and this fact opens the computational possibility of choosing random linear combinations of degenerate states and having some amplitude fluctuations. This is the main purely numerical origin of the finite width of the probability distribution of wave functions of a quasicrystalline system. On the other hand, relatively large disordered systems show some tendency towards localization. Its numerical manifestation is just the increased distribution tail (large am-

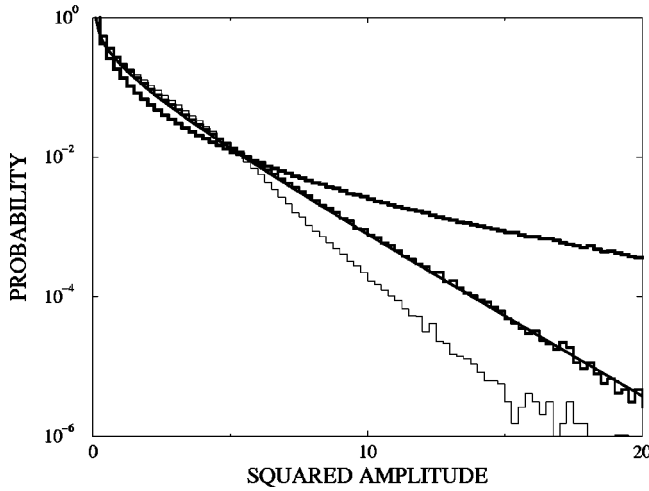


FIG. 3. Wave function statistics as a function of the number of vacancies. Squared amplitude is given relative to its mean value. Statistics are calculated for 1/13 of the total number of states of a 100×100 clusters with 5 (thin stair), 103 (thick stair), and 1992 (thicker stair) vacancies at random positions. Porter-Thomas distribution describing GOE wave function probability distribution is also shown (thick line).

plitude values are allowed for localized states). Similar results are obtained for smaller systems and/or different disorder realizations. Therefore, we are allowed to conclude that measurable deviations from Porter-Thomas statistics are not present in our two-dimensional billiard. Let us remind one that Porter-Thomas statistics excludes the possibility of a fractal character of wave functions, a result that is in agreement with the conclusions attained in the study of our original model [7]. Going a step further, we can say that any weak localization manifestation is absent from our model at the studied length scales. The wave function statistics found in our billiard model should be contrasted with the one proved for two-dimensional metals in the diffusion regime ($l \ll L < \xi$) [13]. In the last case, pre-localized states give rise both to extended tails in the distribution and inverse participation numbers signaling a multifractal behavior of wave functions.

Further analysis of wave function statistics comes from the study of finite size effects for the inverse participation ratio. Results are summarized in Table I. We see that fluctuations about spatial uniformity of eigenfunctions of our model follow the same trend as GOE wave vectors obtained for matrices of the same order. Namely, the relative fluctuation $\delta P_2/P_2$ decreases as $1/L$, L being the square root of the matrices order [14]. Therefore, although fluctuations are a bit larger for our model billiard, exotic dependences such as the $\ln L$ linear dependence proposed by Blanter, Mirlin, and Muzykantskii in [9] can be disproved from our numerical results. Notice that such kind of deviations from GOE statistics would also imply deviations from Porter-Thomas law that we have not observed.

Let us now turn to transport properties of the model under study. To this end, we open to opposite sides of the square cluster and connect them to two ideal leads of width L through hopping integrals equal to bulk values (that is, -1). Kubo formalism is used to calculate the conductance of several samples of increasing sizes [15]. Results are shown in Fig. 4 for two values of the Fermi energy, one very

TABLE I. Finite size effects of the inverse participation ratio P_2 and its fluctuation as obtained for a large number (≈ 5000) of eigenvectors corresponding to the Gaussian orthogonal ensemble and our billiard model.

GOE			
L	$P_2 \times L^2$	$\frac{\delta P_2}{P_2}$	$\frac{\delta P_2}{P_2} \times L$
16	2.9328	0.096835	1.549
32	2.9816	0.049701	1.590
64	2.9960	0.025584	1.637
Our model			
L	$P_2 \times L^2$	$\frac{\delta P_2}{P_2}$	$\frac{\delta P_2}{P_2} \times L$
16	2.9281	0.118610	1.898
32	2.9923	0.070508	2.256
64	2.9996	0.038744	2.480

close to the band center and the second roughly at $\frac{3}{4}$ of the bandwidth. A nice linear behavior is obtained for both energy values up to cluster sizes as large as 500×500 . Conductance fluctuations are also shown in the figure and are typically a small number of times the quantum conductance unit (e^2/h). The meaning of this scaling behavior is unambiguous: our model shows ballistic transport behavior. The linear increase is just reflecting the linear increase in the number of channels, whereas the typical linear decrease along the electrical field direction is absent (Ohm's law predicts a constant value of the conductance in two-dimensional diffusive systems. See an example of diffusive behavior in Fig. 4).

Ballistic transport characteristics could have been inferred from the scaling behavior of the mean free path. Using the

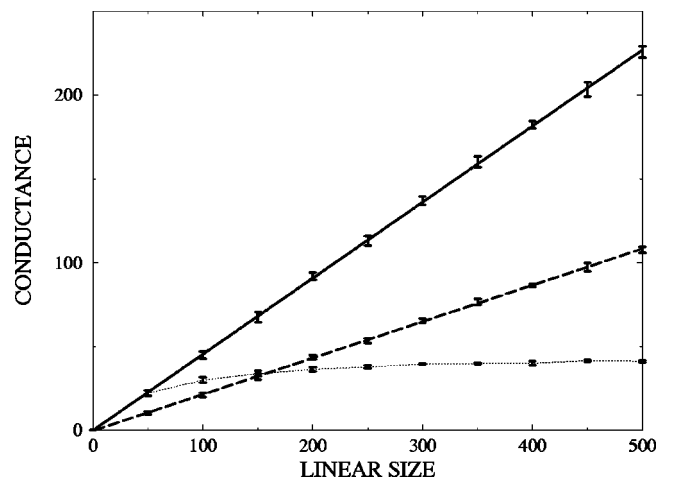


FIG. 4. Scaling of the billiard conductance in e^2/h units as a function of the linear size of the system. Fermi energy is $E = 0.1751$ for the thick continuous line and $E = 2.24399$ for the thick long dashed line. The thin dotted line shows the typical conductance behavior of a diffusive system: Fermi energy is $E = 0.1751$ and the number of vacancies is 2%. Error bars measure the typical dispersion of data.

computational scheme reported in [16], a mean free path of the order of the cluster size ($l \sim 0.6L$ for $E = -2.18$ and L randomly distributed vacancies) is obtained. Actually, whenever the number of vacancies is cL , c being a constant, the mean free path is proportional to L/c . This is what can be understood as a ballistic transport behavior, no matter whether the mean free path is larger or smaller than the system linear size.

In summary, statistical and transport properties of a wide class of ballistic billiards have been numerically studied. Statistical properties are well described by the Gaussian orthogonal ensemble except for the level number variance that saturates at ~ 1 for a number of levels larger than the linear size of the system. Exotic behavior of wave functions, like multifractality or presence of pre-localized states, is absent from our study. Conductance increases linearly with the sys-

tem size, an effect related to the increasing number of channels and the absence of decay in the transport direction. Due both to the simplicity of the model and their nice chaotic behavior, we hope that it can be used as a firm basis for a construction of a general theory of quantum chaos beyond random matrix theory. In particular, we plan a thorough numerical study of wave function spatial correlations for which several theoretical predictions exist [5,17–19].

We are thankful to E. Cuevas and A.D. Mirlin for suggesting to us the use of vacancies and adatoms at the surface of the billiard as a way to simulate roughness in a realistic fashion. This work was supported in part by the Spanish CICYT (Grant No. PB96-0085) and the European TMR Network-Fractals Contract No. FM-RXCT980183.

-
- [1] C.W.J. Beenakker, *Rev. Mod. Phys.* **69**, 731 (1997).
 [2] T. Guhr, A. Müller-Groeling, and H.A. Weidenmüller, *Phys. Rep.* **299**, 189 (1998).
 [3] M.L. Mehta, *Random Matrices* (Academic, New York, 1991).
 [4] K.B. Efetov, *Adv. Phys.* **32**, 53 (1983); *Supersymmetry in Disorder and Chaos* (Cambridge University Press, Cambridge, 1997).
 [5] See, among others, A.V. Andreev and B.L. Altshuler, *Phys. Rev. Lett.* **75**, 902 (1995); Y.V. Fyodorov and A.D. Mirlin, *Phys. Rev. B* **51**, 13 403 (1995); V.I. Fal'ko and K.B. Efetov, *ibid.* **52**, 17 413 (1995).
 [6] N. Pavloff and M.S. Hansen, *Z. Phys. D* **24**, 57 (1992).
 [7] E. Cuevas, E. Louis, and J.A. Vergés, *Phys. Rev. Lett.* **77**, 1970 (1996).
 [8] F. Borgonovi, G. Casati, and B. Li, *Phys. Rev. Lett.* **77**, 4744 (1996); K.M. Frahm and D.L. Shepelyansky, *ibid.* **78**, 1440 (1997); **79**, 1833 (1997).
 [9] Y.M. Blanter, A.D. Mirlin, and B.A. Muzykantskii, *Phys. Rev. Lett.* **80**, 4161 (1998).
 [10] V. Tripathi and D.E. Khmel'nitskii, e-print cond-mat/9802170.
 [11] O. Bohigas, M.J. Giannoni, and C. Schmit, *Phys. Rev. Lett.* **52**, 1 (1984).
 [12] M.V. Berry, *Proc. R. Soc. London, Ser. A* **400**, 229 (1985).
 [13] V.I. Fal'ko and K.B. Efetov, *Phys. Rev. B* **52**, 17 413 (1995).
 [14] Although the values given in the fourth column of Table I are not constant as implied by a strict L^{-1} law, they certainly define a straight line giving the residual L^{-2} dependence.
 [15] The computational implementation of Kubo formula is explained in J.A. Vergés, *Phys. Rev. B* **57**, 870 (1998), and made available in J.A. Vergés, *Comput. Phys. Commun.* (to be published).
 [16] E. Louis, E. Cuevas, J.A. Vergés, and M. Ortuño, *Phys. Rev. B* **56**, 2120 (1997).
 [17] V.N. Prigodin, *Phys. Rev. Lett.* **74**, 1566 (1995).
 [18] Y.M. Blanter and A.D. Mirlin, *Phys. Rev. E* **55**, 6514 (1997).
 [19] S. Hortikar and M. Srednicki, *Phys. Rev. Lett.* **80**, 1646 (1998).